ACADEMIC PRESS

Available online at www.sciencedirect.com

SCIENCE DIRECT®

Journal of Sound and Vibration 263 (2003) 85–111

JOURNAL OF SOUND AND VIBRATION

www.elsevier.com/locate/jsvi

Surface quality monitoring for process control by on-line vibration analysis using an adaptive spline wavelet algorithm

G.Y. Luo*, D. Osypiw, M. Irle

Faculty of Technology, Buckinghamshire Chilterns University College, Queen Alexandra Road, High Wycombe, Buckinghamshire HP11 2JZ, UK

Received 20 March 2001; accepted 10 May 2002

Abstract

The dynamic behaviour of wood machining processes affects the surface finish quality of machined workpieces. In order to meet the requirements of increased production efficiency and improved product quality, surface quality information is needed for enhanced process control. However, current methods using high price devices or sophisticated designs, may not be suitable for industrial real-time application. This paper presents a novel approach of surface quality evaluation by on-line vibration analysis using an adaptive spline wavelet algorithm, which is based on the excellent time–frequency localization of B-spline wavelets. A series of experiments have been performed to extract the feature, which is the correlation between the relevant frequency band(s) of vibration with the change of the amplitude and the surface quality. The graphs of the experimental results demonstrate that the change of the amplitude in the selective frequency bands with variable resolution (linear and non-linear) reflects the quality of surface finish, and the root sum square of wavelet power spectrum is a good indication of surface quality. Thus, surface quality can be estimated and quantified at an average level in real time. The results can be used to regulate and optimize the machine's feed speed, maintaining a constant spindle motor speed during cutting. This will lead to higher level control and machining rates while keeping dimensional integrity and surface finish within specification.

1. Introduction

In recent years, improving the machined surface quality of wood materials has become increasingly important in many areas of the woodworking industry. The surface condition of a

*Corresponding author. Fax: +44-1494-605-051.
E-mail address: gaoyong.luo@bcuc.ac.uk (G.Y. Luo).

0022-460X/03/$ - see front matter
PII: S0022-460X(02)01099-4

workpiece affects the service life, appearance and function of the material [1]. Machining a surface that is below quality specifications can result in losses due to wasted material, re-manufacturing time or both. Thus, surface quality becomes a critical element in the production process.

Feng and Mrad [2] proposed that surface finish information could be used in a feedback loop to vary the process parameters, resulting in increased production efficiency and improved product quality. Process models defining functional relationships between machined surface finish and routing process parameters such as table feed speed, spindle speed, and cut geometry are needed as part of the intelligent control. Through the monitoring of surface quality, feedrates, spindle speeds and tool changes all can be optimized, while minimizing the number of rejected parts and maintaining the correct surface quality.

Surface quality is dependent on the wear state of the tool and the properties of the workpiece material as well as on the woodworking process. The surface characteristic that this study is concerned with is roughness. The properties (i.e., roughness) of a machined surface are strongly influenced by the workpiece characteristics such as machinability and rigidity, the process parameters used during machining, and the dynamic characteristics of the machine tool itself. Machines with computer numerical control (CNC) still require that a programmer select the process parameters such as table feedrates and spindle speeds, thus the process still depends on his knowledge and experience [2]. To prevent an unsatisfactory machined surface finish or even cutter breakage, the programmer frequently tends to be conservative in selecting process parameters with respect to material removal rate, which greatly effects the efficiency of the production process. Therefore, characterizing the material local properties of roughness before or during machining and varying the process parameters based on this information can lead to higher machining rates while keeping dimensional integrity and surface finish within specification.

In practice, however, the fundamental data of wood surface quality are accessible mainly by means of rather sophisticated sensors, e.g., laser scanners, vision systems and computer tomography. When compared with metal cutting such as that discussed in Refs. [3–8], where techniques are relatively well-established, it has been shown even more complicated to measure and predict the surface quality of wood composites. Orech et al. [9] proposed the use of lasers for the electro-optical testing of wood surfaces, mainly for identification of some structural wood defects and qualitative evaluation of wood surfaces. An optical profilometer to measure the relative height of the wood surface was developed by Lemaster and Taylor [10]. This device utilizes a laser beam and lateral effect photodiode. Lemaster and Beall [11] also used a laser-based optical profilometer to measure surface roughness of medium density fibreboard (MDF). Fuchs [12] discussed the application of computer vision and pattern analysis for the inspection of wooden materials, such as X-ray computed tomography (CT) for 3-D information on wood surface, and concluded that for the most practical applications such techniques are outside the economic limits of today. Faust [13] described that stylus tracing is a suitable technique for laboratory work, but is generally inadequate for measuring roughness at production rates due to the slow travel speed. A method using a video camera with image analysis is proposed in his work by correlating it with stylus tracing and visual classification techniques. However, the speed of the measurement is constrained by the complexity of the computing algorithm.

The high cost of measurement devices or their sophisticated designs do not make them suitable for industrial real-time application, that is one of the major factors why the wood machining automation has been one step behind many other industrial branches. The effort of this paper is to

propose a potential solution by vibration analysis with a developed wavelet algorithm. This will provide a possibility of optimizing process control.

2. Vibration and surface quality

2.1. Theoretical calculation of surface quality

When machining, each cutter strikes the workpiece, and leaves a knife mark on the surface. Generally, the marks are assumed to be arcs. The final surface consists of a number of closely spaced arcs (see Fig. 1), merging with each other to give the appearance of a truly flat surface. The surfaces can be graded according to the pitch of cutter marks, which is measured from crest to crest of each arc (as shown in Fig. 1, in which the horizontal axis denotes feeding and the vertical axis denotes rotation). The longer the pitch the less flat the surface will be. It is usual, when calculating, to assume that all cutters set on a block cut equally and all leave marks on the surface. The pitch of cut marks can then be calculated [14]

$$P = \frac{1000F}{NR}, \tag{1}$$

where F is the feed speed (m/min), N the number of cutter teeth set to identical cutting circle, P the pitch of cutter mark (mm) and R the revolutions per minute of the cutter block (r.p.m.).

In the general case in which all other factors remain constant, an increase in feed speed increases the instantaneous radius of curvature of the knife path, the height of the individual knife marks,

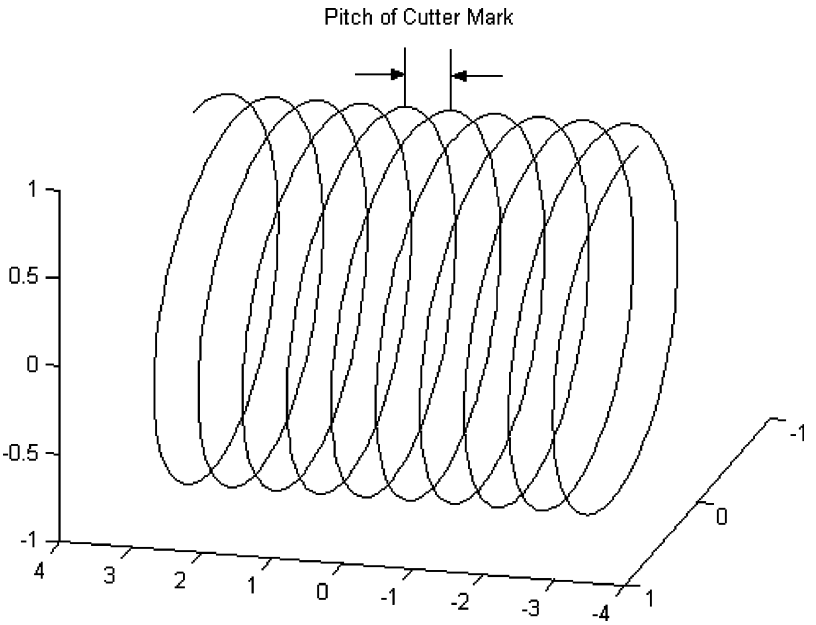

Fig. 1. The pitch of cutter mark.

and the distance between knife marks. The last two effects are detrimental to surface quality as feed speed increases [15].

R can be calculated from the motor speed as

$$R = R_m \times (1 - 5\%) = R_m \times 95\%, \tag{2}$$

where R_m is the motor speed.

The explanation for this is that the squirrel cage induction motors, commonly used to drive the woodworking machine, run at approximately 95% of the rotation of the magnetic flux [14].

Define $f = NR/60$, as the number of cuts occurring each second, then one obtains the fundamental frequency relating to pitch of the cutter mark, which is an indicator of surface quality. This frequency and its harmonics, and their side bands in the vibration signals may generally be correlated to surface quality.

Although the speed theory successfully describes cutting behaviour of machining process with respect to surface quality, the correlation between vibration, which is common in any rotating and moving machines, and the surface quality has not been adequately addressed.

2.2. Vibration in machining process

The dynamic behaviour of the wood machining process plays an important role for the surface finish quality of machined workpiece. The superposition of the rotational cutting motion and the varying feed movement results in cycloidal grooves on the workpiece surface. The groove (pitch) width depends on the feed per revolution, while irregularities of the groove pattern are either a result of vibrations during cutting or of unequal tooth radiuses [16].

In any woodworking machinery, vibrations during machining generally cause a periodic change of the relative position between workpiece and tool, and result in a modified surface texture or in a dimensional error. This may lead to a deficient surface quality, depending on the chosen process parameters and the machine's dynamic behaviour. For any dynamic optimization of machining process with focus on an increased surface quality, exact knowledge of those vibration components that influence the surface quality is needed. A vibration's influence on the surface quality does not exclusively depend on its amplitude [16]. As previously discussed, the frequency bands, which are related to the rotating frequency of the cutter (or the fundamental frequency), may also correlate with the quality of the surface pattern. In addition, Heisel and Krondorfer [17] have noticed that the unbalance vibration is usually so large that only one tooth is actually involved in cutting (one knife finish). The signature of unbalance vibration normally has the form of amplitude along the rotating frequency and its harmonics. Since in any machine with rotating members, complete balancing of any rotating member is impossible [18], the rotating frequency and its harmonics should be considered as the components which influence the surface quality. However, high-frequency components of vibration (larger than 5 times the rotating frequency) are normally of very small amplitude and can therefore be ruled out as a cause of reduced surface quality [17].

Vibration analysis can provide a quick and relatively easy way to extract information that may relate to surface quality. However, it is still a challenge to isolate and characterize only those specific signatures relevant from the vibration signals for the evaluation of surface quality. This paper presents a novel approach of vibration signal analysis with a fast wavelet algorithm, to

establish a link between surface quality and vibration energy in the time domain, which represents the change of amplitude in the multiple frequency bands determined by wavelet analysis.

2.3. Methods of vibration analysis

For vibration analysis there are economical sensors available that are easy to mount, and the acquisition, transmission and storage of data can be easily handled. This makes on-line remote monitoring possible, using a variety of signal processing algorithms on the measured vibration signals. Vibration signals are considered as non-stationary with transient signals. The frequency characteristics of vibration signals are time-varying. Fig. 2 is an example of a vibration signal measured from a machine spindle and Fig. 3 is its power spectrum. Non-stationary analysis techniques have received particular attention. As a result there are many spectral analysis techniques, which have been fully developed and established over the years for processing the raw measured vibration signals. These techniques include short-time Fourier transform (STFT), Wigner–Ville distribution (WVD) or autoregressive (AR) method.

The STFT is computationally efficient, but has the drawback that the choice of the window length simultaneously affects both frequency and time resolution: for a good frequency resolution a high window length has to be chosen, but this choice detrimentally affects time resolution [19]. WVD can overcome these limitations; however, it has a different drawback in that the time–frequency analyses are signal dependent and perform better or worse depending on the signals, mainly because of the so-called cross-term interference. WVD introduces cross-terms when signals with multifrequency components are analyzed [20]. If the bandwidths of the components in a

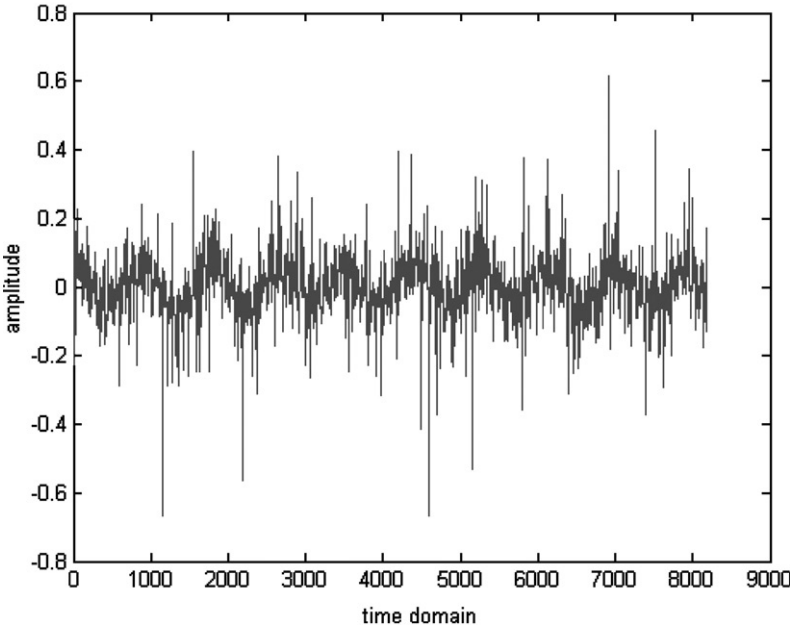

Fig. 2. An example of vibration signal.

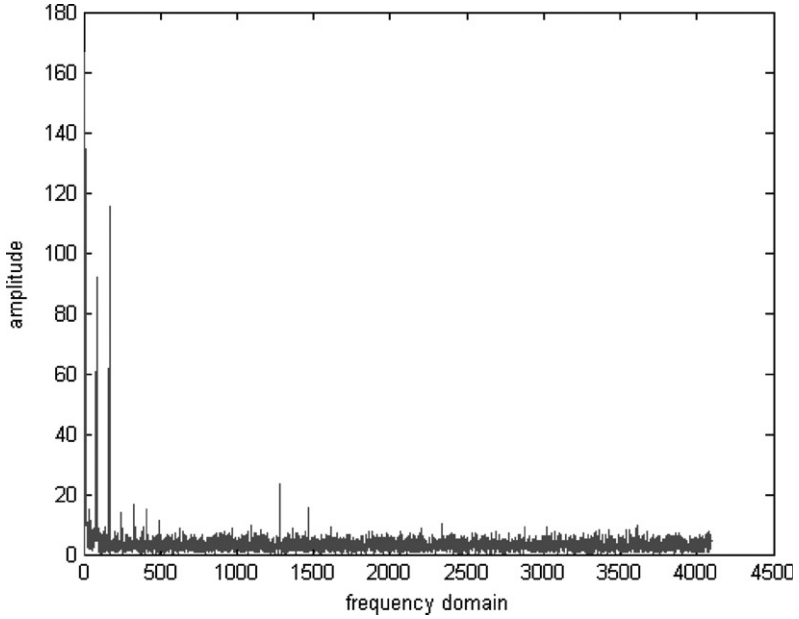

Fig. 3. Power spectrum of the vibration signal.

multicomponent signal are overlapped, certain cross-interference (cross-term) reduction techniques must be applied, and that leads to the reduction of resolution. AR models have been widely used for time–frequency analysis, but mainly suitable for stationary signals or for the case of slowly varying spectra [19].

However, the newly developed wavelet transform allows analysis of a signal or parameterization of a signal that can locate energy in both time and scale (or frequency) domain within the constraints of uncertainty principle. This property makes it very suitable for the detection of vibration transients. The application of wavelet transform in time–scale and time–frequency analysis has been proven to be a useful tool for the detection and characterization of vibration transients [21,22]. However, current methods with discrete or continuous wavelet transforms (CWT) have either low resolution of features in frequency-band scale for detailed analysis or are very time consuming [23]. The main problem in time–frequency wavelet analysis is to obtain a good and flexible frequency resolution with its evolution over time in less computing time, making it possible for real-time application

3. Adaptive spline wavelet algorithm

3.1. Wavelet analysis

Wavelets are new basis functions, derived from one mother wavelet by dilation and translation [24]. Wavelet analyses decompose data into different frequency components, and then study a component with a resolution matched to its scale. This is based on low frequencies with more

frequency resolution and less time resolution than high frequencies, and vice versa. They have advantages over traditional Fourier methods in analyzing non-stationary signals.

The wavelet transform (WT) is defined as the inner product of the signal $x(t)$ with a two-parameter family of basis function

$$WT(b,a) = |a|^{-1/2} \int_{-\infty}^{\infty} x(t)\bar{\psi}\left(\frac{t-b}{a}\right) \mathrm{d}t, \tag{3}$$

where $\psi_{b,a} = \psi((t-b)/a)$ is an oscillatory function, $\bar{\psi}$ denotes the complex conjugate of ψ, b is the time delay (translation parameter) which gives the position of the wavelet, a is the scale factor (dilation parameter) which determines the frequency content. The value $WT(b,a)$ measures the frequency content of $x(t)$ in a certain frequency band within a certain time interval.

The form of Eq. (3) is a CWT. It is calculated by continuously shifting a continuously scalable function over a signal and calculating the correlation between the two. From a computational point of view, this transform is not efficient. One way to solve this problem is to sample the CWT on a two-dimensional grid $(a_j, b_{j,k})$ [25]. In Eq. (3), if the dyadic scales $a_j = 2^j$ are chosen, and if one chooses $b_{j,k} = k2^j$ to adapt to the scale factor a_j, one obtains

$$d_{j,k} = WT(k2^j, 2^j) = |2^j|^{-1/2} \int_{-\infty}^{\infty} x(t)\bar{\psi}\left(\frac{t-k2^j}{2^j}\right) \mathrm{d}t = \langle x(t), \psi_{j,k}(t) \rangle, \tag{4}$$

where $\psi_{j,k}(t) = 2^{-j/2}\psi(2^{-j}t - k)$.

This is the form of a discrete wavelet transform (DWT). The wavelet coefficients $d_{j,k}$ are considered as a time–frequency map of the original signal $x(t)$.

The driving impetus behind wavelet analysis is their property of being localized in time (space) as well as scale (frequency). Because of the time–frequency localization of wavelets, efficient representations of signals can be obtained. Wavelets initiated by Daubechies [26] involve constructing the filters that are used in the fast wavelet transform, with filter banks called low- and high-pass filters [27]. These filters are constructed from a wavelet basis which starts with the construction of a scaling function [28]. This leads to multiresolution analysis, in which a scaling function behaves as a low-pass filter and a wavelet function as a high-pass filter (or band-pass filter).

Classical wavelet basis is generally given by the set of dyadic dilated (index j) and translated (index k) versions of one fixed mother wavelet as $\{\psi_{j,k}(t) = 2^{-j/2}\psi(2^{-j}t - k)\}_{(j,k)\in Z^2}$. However, the dyadic dilation and translation DWT cannot compactly represent signals with a narrow high-frequency support. This may produce low resolution of features in frequency-band scale for detailed analysis. This paper presents adaptive spline wavelet filter design for on-line vibration general and detailed analysis.

3.2. Battle–Lemarié wavelet filter design

Splines have many nice properties that have contributed to their recent popularity for constructing wavelet bases and multiresolution signal analysis [29–35]. In wavelet theory, splines constitute a case apart because they give rise to the only wavelets that have a closed-form formula [36]. Of particular interest are the B-spline wavelets, which are compactly supported, and

offer close-to-optimal time–frequency localization in the sense specified by the uncertainty principle [37].

The Battle–Lemarié wavelets are constructed by orthogonalizing B-spline functions [38]. They also have the advantage of symmetry and, more importantly, an approximate closed-form representation can be obtained by decomposing the wavelets into B-spline or polynomials of the same order. The development of the Battle–Lemarié wavelets begins with defining an appropriate scaling function ϕ that generates a multiresolution analysis, and then constructs corresponding wavelets.

The mth-order Lemarié–Meyer wavelet is constructed from a linear combination of the translations of the mth-order B-spline function $B_m(t)$ [39]. The Fourier transform of $B_m(t)$ is

$$B_m(\omega) = \mathrm{e}^{-\mathrm{i}m\omega/2}\left(\frac{\sin(\omega/2)}{\omega/2}\right)^{m+1}. \tag{5}$$

After performing orthonormalization, the scaling function $\phi(t)$ can be obtained by finding the inverse Fourier transform of

$$\phi(\omega) = \mathrm{e}^{-\mathrm{i}N\omega/2}\left(\frac{\sin(\omega/2)}{\omega/2}\right)^{m+1} s_m^{-1/2}(\omega), \tag{6}$$

where $N = 0$ if m is odd, or $N = 1$ if m is even, with

$$s_m(\omega) = \sum_k |B_m(\omega + 2\pi k)|^2.$$

Since the time–frequency property of cubic spline is near optimal [40] and can suit most practical cases, $m = 3$ is chosen in this study. Thus

$$s_3(\omega) = (64\cos^6(\omega) + 1824\cos^4(\omega) + 2880\cos^2(\omega) + 272)/5440.$$

The orthonormal wavelet $\psi(t)$ can be obtained from its Fourier transform [39]

$$\psi(\omega) = \mathrm{e}^{-\mathrm{i}\omega/2}\bar{\eta}_0\left(\frac{\omega}{2} + \pi\right)\phi(\omega), \tag{7}$$

where the overline on η_0 denotes the complex conjugate and $\eta_0(\omega/2) = \phi(\omega)/\phi(\omega/2)$.

Although all orthonormal wavelets, except the Haar system, do not have an explicit closed form representation, they normally can be represented by the dilation function

$$\phi(t) = \sum_k h_k \phi(2t - k),$$

$$\psi(t) = \sum_k g_k \phi(2t - k), \tag{8}$$

where h is low-pass filter and g is band-pass filter. The scaling function and wavelet are periodic. In the frequency domain, one has

$$\phi(\omega) = h(\omega/2)\phi(\omega/2),$$

$$\psi(\omega) = g(\omega/2)\phi(\omega/2). \tag{9}$$

Hence, the filters can be obtained in physical space for compactly supported bases and in Fourier space through

$$h(\omega) = \phi(2\omega)/\phi(\omega),$$

$$g(\omega) = \psi(2\omega)/\phi(\omega). \tag{10}$$

Because of the orthogonality of the Battle–Lemarié wavelet, the perfect reconstruction of the signal can be achieved [27], which may be used for signal reconstruction and compression. However, in terms of vibration analysis, if signal synthesis is not needed, $a(a > 0)$ may be used as the dilation factor instead of dyadic analysis, thus

$$h(a\omega) = \phi(a2\omega)/\phi(a\omega),$$

$$g(a\omega) = \psi(a2\omega)/\phi(a\omega). \tag{11}$$

By taking inverse Fourier transform

$$F^{-1}\{h(a\omega)\} = \frac{1}{a}h(t/a),$$

$$F^{-1}\{g(a\omega)\} = \frac{1}{a}g(t/a). \tag{12}$$

The filter coefficients are obtained, which can be normalized by multiplying a instead of $a^{-1/2}$.

3.3. Arbitrary fine time–scale representation

Using the previously developed filter bank, and choosing $a = 2^{j-1}2^{l/L}$ $(j = 1, 2, \ldots, J, l = 1, 2, \ldots, L)$, where J, L are the positive integers, then the signal can be decomposed into J levels by non-decimated dyadic analysis (let $l = 0$). That is, at level j: $f_s/2^{j+1} \leqslant f \leqslant f_s/2^j$ and at level J: $0 \leqslant f \leqslant f_s/2^J$. The corresponding multiresolution analysis can be seen in Fig. 4, and Fig. 5 is an example of the time–scale map constructed with $J = 9$ using the vibration signal shown in Figs. 2 and 3.

At level j, the signal can be further decomposed into L levels for more detail. An example is shown in Fig. 6 with $j = 6$ shown in Fig. 5, and $L = 10$.

The dyadic time–scale multiresolution analysis is based on low frequency with more frequency resolution and is suitable for general analysis across the whole frequency range. The frequency band of interest can be further decomposed in arbitrary fine scale. The time–scale representation can provide more detailed information.

3.4. Adaptive frequency resolution decomposition

The signal decomposition in the previous approach is based on the low-frequency resolution at high frequencies and high-frequency resolution at low frequencies. However, in terms of vibration analysis, high-frequency signals also contain very useful information on the process. Therefore, there is a need to achieve high-frequency resolution at high frequencies. This can be obtained by dilating the spline wavelet in the frequency domain and shifting the central frequency. From

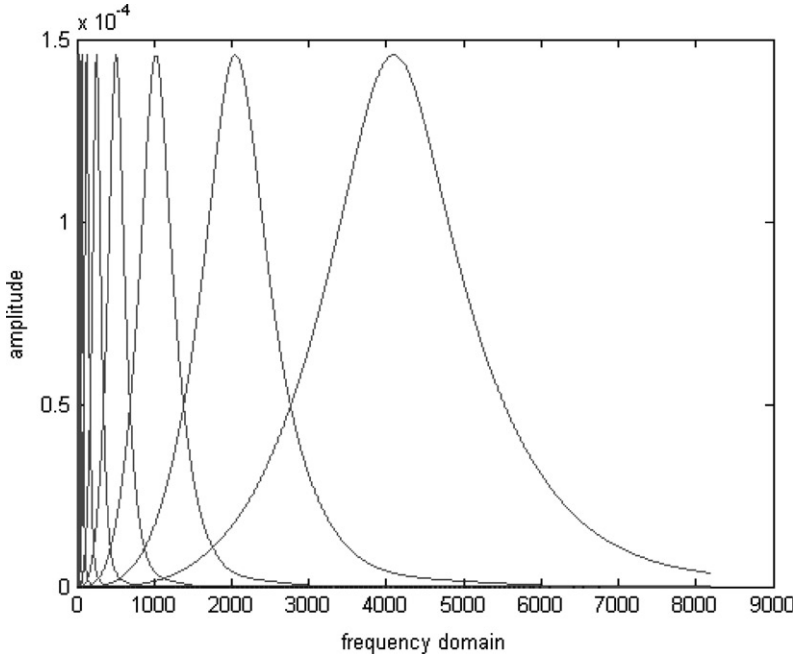

Fig. 4. Dyadic multiresolution analysis of spline wavelet.

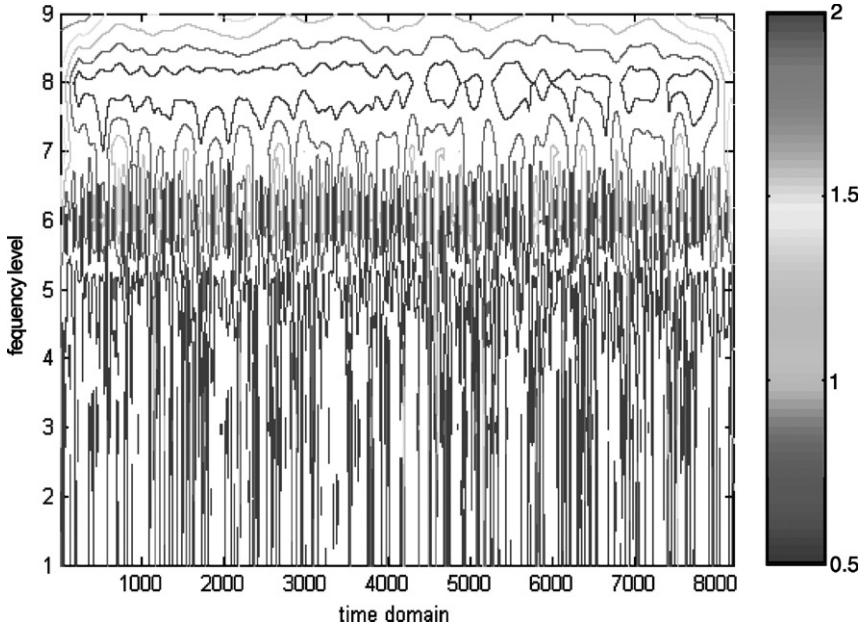

Fig. 5. Time–scale map with $J = 9$.

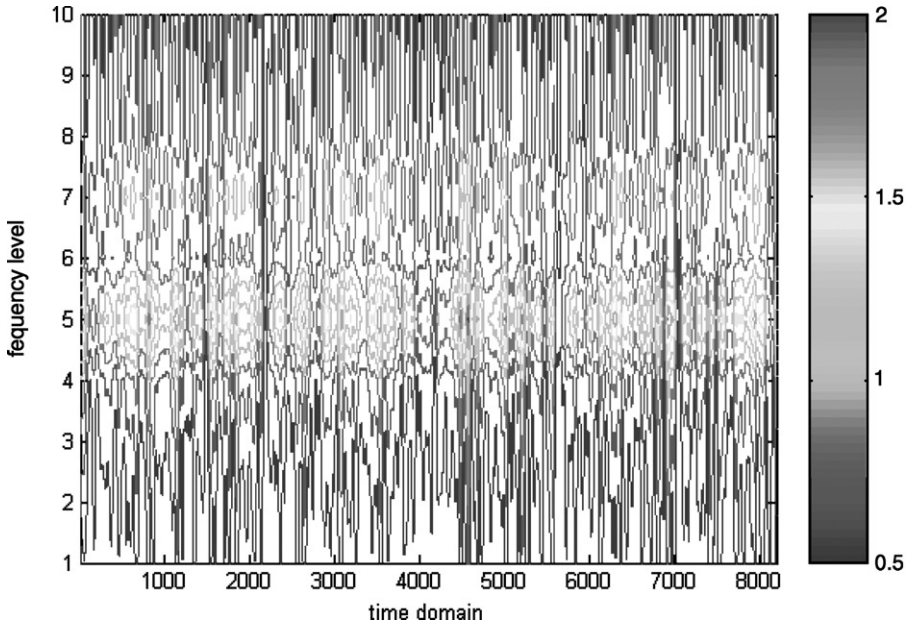

Fig. 6. Time–scale map with $L = 10$.

Eq. (5), one may define

$$\psi_m(a(\omega-\omega_0)) = \mathrm{e}^{-\mathrm{i}ma(\omega-\omega_0)/2}\left(\frac{\sin(a(\omega-\omega_0)/2)}{a(\omega-\omega_0)/2}\right)^{m+1}, \tag{13}$$

where $a \geqslant 1$ and ω_0 is the analyzing central frequency. The wavelet ψ_m behaves as a band-pass filter. The frequency resolution (i.e., bandwidth of the filter) can be approximated by $\Delta\omega \approx 2\pi/a$ when $m = 3$ (within the limitation of uncertainty principle). Although B-spline wavelets converge to the Gabor functions (modulated Gaussians) as m goes infinity, and larger order leads to higher resolution, in most cases the order $m = 3$ is proposed, which possesses near-optimal time–frequency localization property [40]. When very high-resolution analysis is needed, m may be increased.

With this algorithm, by proper selection of a, the resolution can be linear or non-linear. The central frequency is flexible to shift. This can make the decomposition more case-orientation and tailor-made. One can thus take advantage of the convolution theorem to compute the convolution of two functions by using a fast Fourier transform (FFT). However, when bandwidth is very narrow, the FFT method is less precise than convolution, thus a Gaussian wavelet filter can be used [41]. In this study, since the bandwidth is not very narrow and large data sizes are to be analyzed, it is usually more efficient to convert things to the frequency domain and back [42].

By shifting the analyzing central frequency, a single central frequency filter with single band-pass and a multiple central frequencies filter with multiband-pass, can be obtained. To determine the contributions of vibration components correlated to surface quality, a multiple central frequencies filter with adaptive and flexible resolution is used.

The adaptive dilation factor a can vary the resolution as linear or non-linear give high resolution at high-frequency range:

Linear: for example

$$a_k = \frac{2\pi}{\Delta\omega}, \quad k = 1, 2, \ldots, n, \tag{14}$$

where $\Delta\omega$ is the frequency resolution and kept constant, ω_k is the kth analyzing central frequency, and for this example $\omega_k = \omega_0(2k-1)$ is used, $\omega_1 = \omega_0$ is the first analyzing frequency.

Non-linear: for example

$$a_k = \frac{2\pi}{\Delta\omega_{min} k^2}, \quad k = 1, 2, \ldots, n, \tag{15}$$

where $\Delta\omega_{min}$ is the highest resolution corresponding to the first analyzing frequency (highest one). For this example, the choice of $\omega_k = \omega_0(n-k+1)$ will be used. Fig. 7 is an example of a non-linear dilation factor with $n = 8$.

Thus when choosing $m = 3$, one has

$$\psi_k(\omega) = a_k \psi_3(a_k(\omega - \omega_k)). \tag{16}$$

In the case of non-linear resolution, the bigger the k, the lower the ω_k. In other words, the bandwidth is wide at low frequency, and narrow at high frequency. To calculate all contributions of these n bands to the feature of the vibration signal

$$\psi(\omega) = \sum_{k=1}^{n} \psi_k(\omega) \tag{17}$$

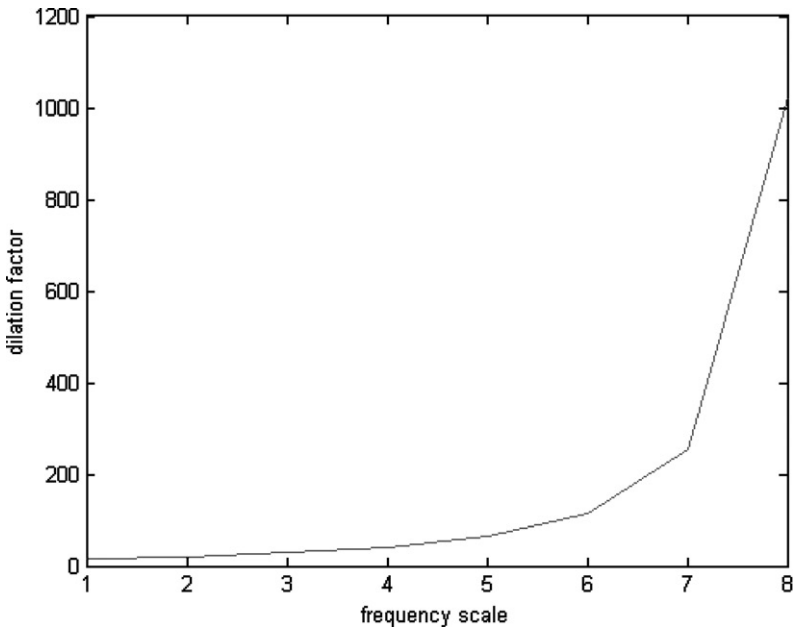

Fig. 7. An example of non-linear dilation factor.

and the wavelet transform can be expressed in the frequency domain

$$WT(\omega) = x(\omega)\psi(\omega). \tag{18}$$

In the time domain the summation of the contribution can be defined as root sum square (RSS):

$$RSS = \sqrt{\sum_{i=1}^{L} |WT(t_i)|^2}, \tag{19}$$

where $WT(t) = F^{-1}\{WT(\omega)\}$, F^{-1} denoting the operation of inverse transform of the power spectrum, L is the signal length, and $|WT(t_i)|$ is defined as the wavelet power spectrum at time t_i. RSS values are used as indication of surface quality.

4. Methodology of experiment

The experimental set-up is shown in Fig. 8. A RYE MA 1500 CNC Router machine tool was used in this experiment, which can cut wood, plastics, non-ferrous materials and composites. The routing spindle has a power rating of 7.5 kW, a speed range 0–24 000 r.p.m. split into 11 levels, driven by a three-phase motor with a squirrel cage rotor. The cutting tools used were Tungsten Carbide Tipped (TCT) panel cutters with a diameter 10 mm, as shown in Fig. 9. Spindle vibrations were measured using non-contacting eddy current probes (Sensonics EC1/EC4 series eddy current probe system). The analogue signals were sampled with a PCI-bus compatible data-acquisition board (PCI-DAS1200, ComputerBoards, Inc.) installed in one expansion slot of the microcomputer. The sampling rate was $f_s = 30\,120$ Hz. The tests are performed under different cutting conditions. Spindle speed, feed speed, tool wear and depth of cut are varied, and the corresponding vibration signals are sampled.

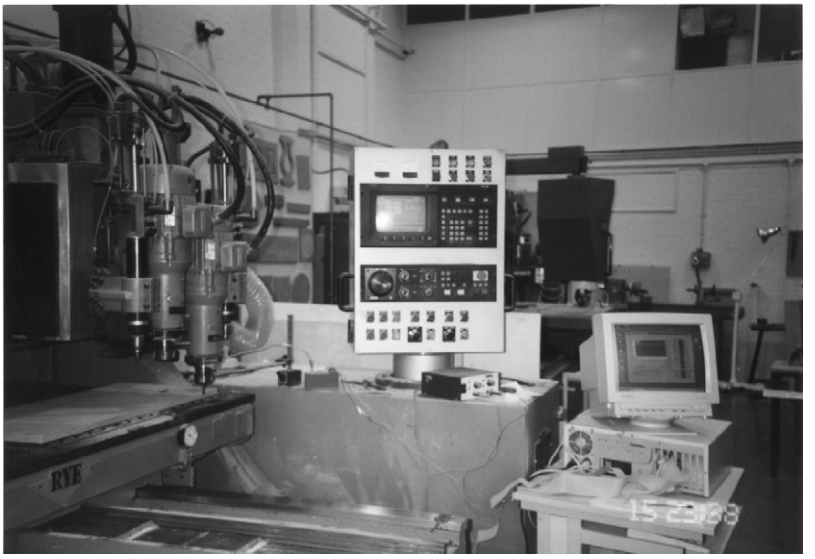

Fig. 8. The test rig.

Fig. 9. TCT panel cutters with different tool wear states.

Table 1
Tests with varying feed speed

Test no.	Spindle speed (r.p.m.)	Feed speed (m/min)	Depth of cut (mm)
1, 2, 3, 4, 5	Level 11	0.5, 1, 1.5, 2, 2.5	7
6, 7, 8, 9, 10	Level 9	0.5, 1, 1.5, 2, 2.5	5
11, 12, 13, 14, 15	Level 6	0.5, 1, 1.5, 2, 2.5	3
16, 17, 18, 19, 20	Level 11	0.5, 1, 1.5, 2, 2.5	5
21, 22, 23, 24, 25	Level 9	0.5, 1, 1.5, 2, 2.5	3
26, 27, 28, 29	Level 6	2.5, 5, 7.5, 10	3

Note: Spindle speed = (2400 × level/11)(r.p.m.).
Feed speed corresponding to test no., such as 0.5 m/min to test no. 1. The condition of the tool is classed as slight wear for these tests.

So far an accepted and unified quantitative method to measure the surface quality of wood composites has not been established [43]. In this study, after machining, the surface was scanned using a Talyscan 150 laser triangulation to measure the roughness of surface finish. The inverse proportion of average roughness (R_a) was used as an indication of surface quality, since average roughness is a widely used roughness parameter for wood finish [43–46]. On the other hand, the demand for MDF has recently increased because of its easiness of processing. However, the machinability of MDF has not been investigated sufficiently [47]. Thus in this study, MDF was chosen as the workpiece material. Two MDF boards were used with dimensions

$$\text{Board 1:} \quad 1475 \times 1220 \times 20\,\text{mm}^3,$$

$$\text{Board 2:} \quad 470 \times 300 \times 25\,\text{mm}^3.$$

Table 2
Tests with varying tool wear

Test no.	Spindle speed (rpm)	Tool wear state	Depth of cut (mm)
30, 31, 32, 33, 34	Level 11	a, b, c, d, e	7
35, 36, 37, 38, 39	Level 9	a, b, c, d, e	5

Note: Feed speeds are: (1) at level 11 (test nos. 30–34), 3.0 m/min; (2) at level 9 (test nos. 35–39), 2.0 m/min.

Table 3
Tests for measurement of surface roughness

Test no.	Spindle speed (r.p.m.)	Feed speed (m/min)	Depth of cut (mm)
40, 41, 42, 43, 44	Level 11	0.5, 1, 1.5, 2, 2.5	7
45, 46, 47, 48, 49	Level 9	0.5, 1, 1.5, 2, 2.5	3

Note: Measured using a Talyscan 150 laser triangulation.

These boards were machine cut and their surface roughness was measured. To do this, a series of experiments were conducted, these are shown in Tables 1–3. Vibration signals at free running were also recorded at each rotating speed. The tests in Tables 1 and 2 are performed with varying feed speed (Board 1) and varying tool wear (Board 2), respectively. Tool wear states are defined according to average flank wear of cutting tool [48]: (a) sharp tool, (b) slight wear, (c) medium wear, (d) severe wear, and (e) breakage. The feed speeds in Table 2 are: at level 11, 3.0 m/min and at level 9, 2.0 m/min. Tests shown in Table 3 are for the measurements of surface roughness.

5. Results and discussion

5.1. Experimental results

The signals recorded during the experiments listed in Tables 1–3 are analyzed in order to determine the contributions of vibration components to surface quality. The analysis is carried out off-line but with a view to on-line implementation of monitoring system using the fast wavelet algorithm.

Fig. 2 shows a vibration signal measured with the machine free running (under no load condition). The speed of driving motor is at speed 9 level. The number of cutter teeth is $N = 2$. Thus, the fundamental frequency can be calculated as

$$R_m = \frac{24\,000 \times 9}{11} \approx 19636 \text{ r.p.m.},$$

$$R = R_m \times 95\% \approx 18655 \text{ r.p.m.}$$

Therefore, the fundamental frequency

$$f = \frac{NR}{60} = \frac{2 \times 18\,655}{60} \approx 622 \text{ Hz}$$

and the rotating frequency

$$f_r = \frac{R}{60} = \frac{18\,655}{60} \approx 311 \text{ Hz}.$$

For general analysis, an arbitrary fine scale analysis of spline wavelet can be used. Fig. 5 is the contour plot with $l = 0$, and $J = 9$ calculated from the original signal shown in Fig. 2. It can be seen that there are strong signals at level 5 (frequency range 941–471 Hz) and level 6 (frequency range 235–471 Hz), within which may be the fundamental frequency or rotating frequency. Thus, the signal at level 6 is further decomposed into $L = 10$ levels, which is shown in Fig. 6. A strong signal can be seen at level 5, of which the central analyzing frequency is around 309 Hz. This is very close to the above calculation. The adaptive spline wavelet algorithm with higher resolution can be used to analyze the signal in time–frequency map for further detail. The aim is to look for spectrum peaks with spacings equal to the nominal and thereby obtain an accurate estimation of fundamental frequency and rotating frequency. The search for peaks takes place at a frequency range, which is determined by the theoretical calculation and the general analysis of the signal. The signal with frequency range 0–735 Hz thus is decomposed into 20 levels. The filters are shown in Fig. 10 with the frequency resolution chosen to be the same at each level. Fig. 11 shows the corresponding time–scale map. It can be seen that there are two strong signals at level 9 (294–331 Hz) and level 17 (588–625 Hz) with equal spacing. These are the ranges of rotating and fundamental frequency. Thus using the method described in Ref. [49], the frequencies can be accurately identified: $f_r = 305$ Hz and $f = 610$ Hz.

As discussed earlier, rotating frequency and the cutter frequency (fundamental frequency), and their harmonics and the side band families, may all contribute to surface quality. Thus, a series of

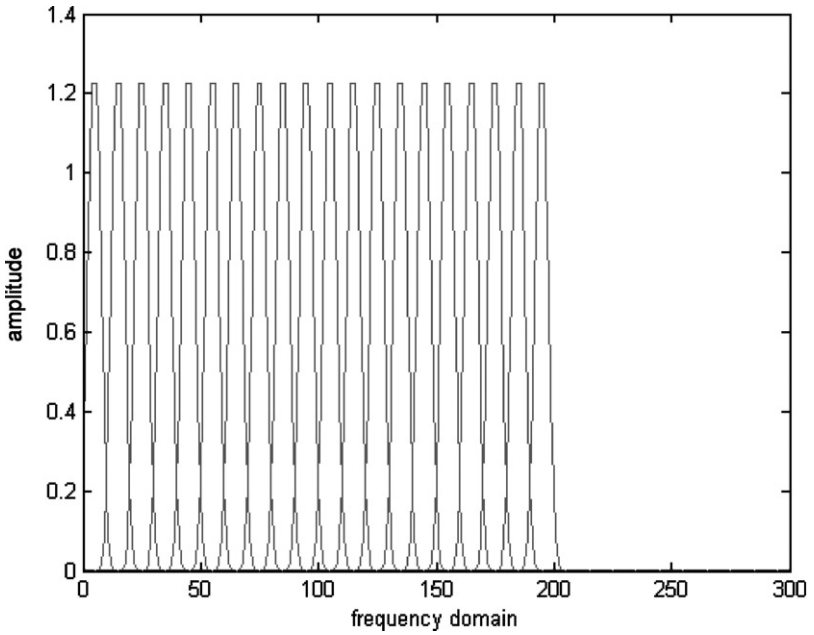

Fig. 10. Filters in the frequency domain for 20 levels.

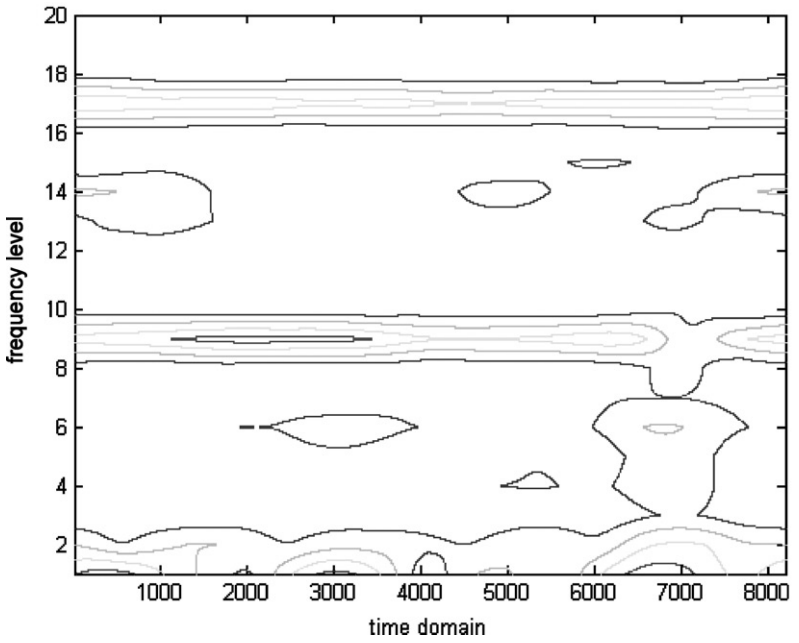

Fig. 11. Time–scale map with frequency range 0–725 Hz.

adaptive resolution filters with variable bandwidth were used to calculate the contributions (RSS of wavelet power spectrum) in the time domain. Both filters of linear and non-linear resolution were used to process the vibration signals measured from the experiments with the aim of identifying those features that contribute to surface quality. The best filter with linear resolution was found to be $\Delta f = 37$ Hz, $f_0 = 305$ Hz, $n = 8$, for the representation of unbalance (rotating frequency) components' influence. And the best filter with non-linear resolution was $\Delta f_{min} = 37$ Hz, $f_0 = 610$ Hz, $n = 8$, for cutting behaviour (fundamental frequency) analysis. In order to reduce computing time, the two filters were combined into a single filter as shown in Fig. 12 in the frequency domain with amplitude being normalized. An example vibration signal measured when running at the speed of level 9 and feed speed 0.5 m/min (test no. 21) is shown in Fig. 13. The results (RSS values and the inverse proportion of average roughness) are summarized as follows:

(i) Results of tests described in Tables 1 and 2: Test results corresponding to Tables 1 and 2 are listed in Table 4. The results are shown in the form of graphs, listed as figures in the table. From these figures (Figs. 14–18), the variation of the surface quality using RSS values can be clearly seen.

(ii) Results of tests described in Table 3: For speed level 11, an example of surface roughness profile corresponding to test no. 40 is shown in Fig. 19. The results shown in Fig. 20 are the surface quality calculated from roughness measurement test nos. 40–44 (corresponding to cutting test nos. 1–5). For speed level 9, an example of surface roughness profile corresponding to test no. 46 is shown in Fig. 21. The results shown in Fig. 22 are the surface quality calculated from roughness measurement test nos. 45–49 (corresponding to cutting test nos. 21–25).

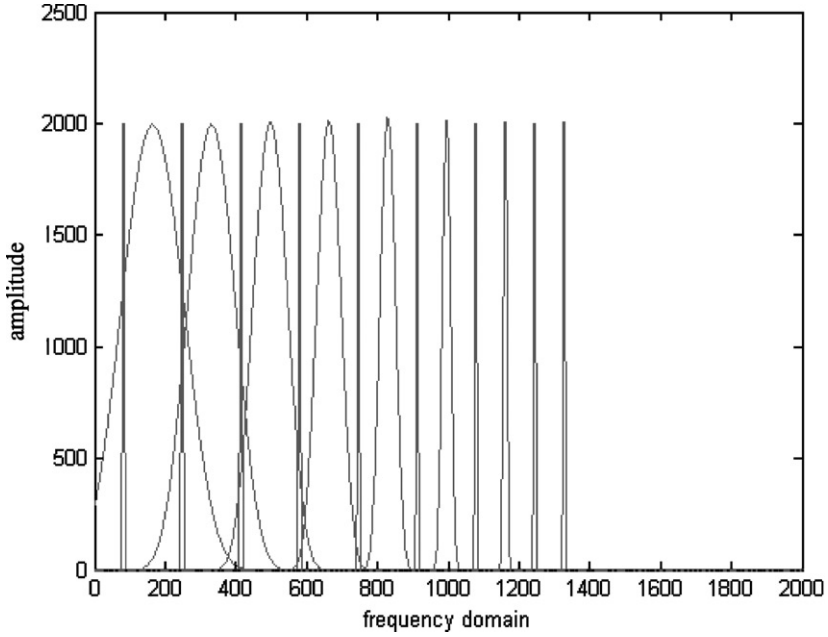

Fig. 12. Summation of filters with amplitude being normalized.

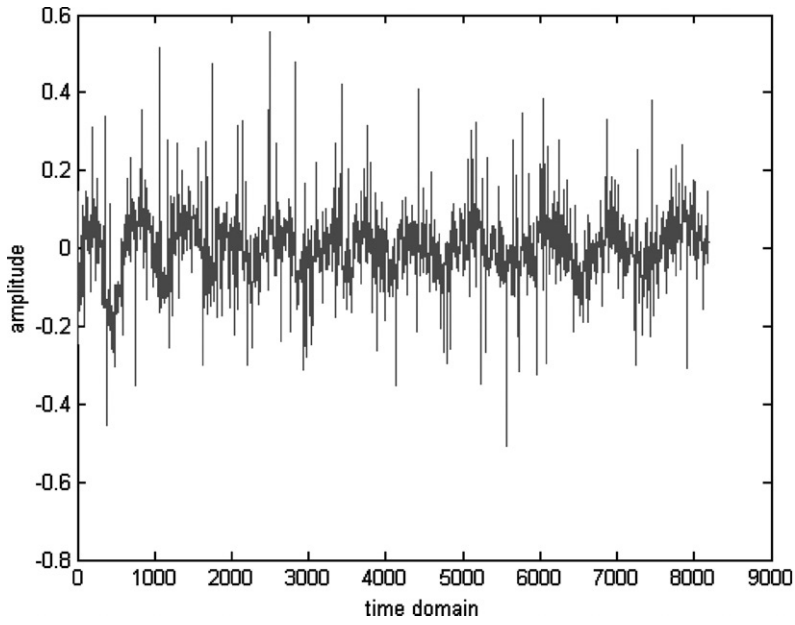

Fig. 13. Vibration signal measured with running at speed level 9 (test no. 21).

Table 4
Test results corresponding to Tables 1 and 2

Spindle speed (level)	Test no.	Results shown
9	6–10, 21–25	Fig. 14
11	1–5, 16–20	Fig. 14
6	11–15	Fig. 14
11	1–5	Fig. 15
6	26–29	Fig. 16
11	30–34	Fig. 17
9	35–39	Fig. 18

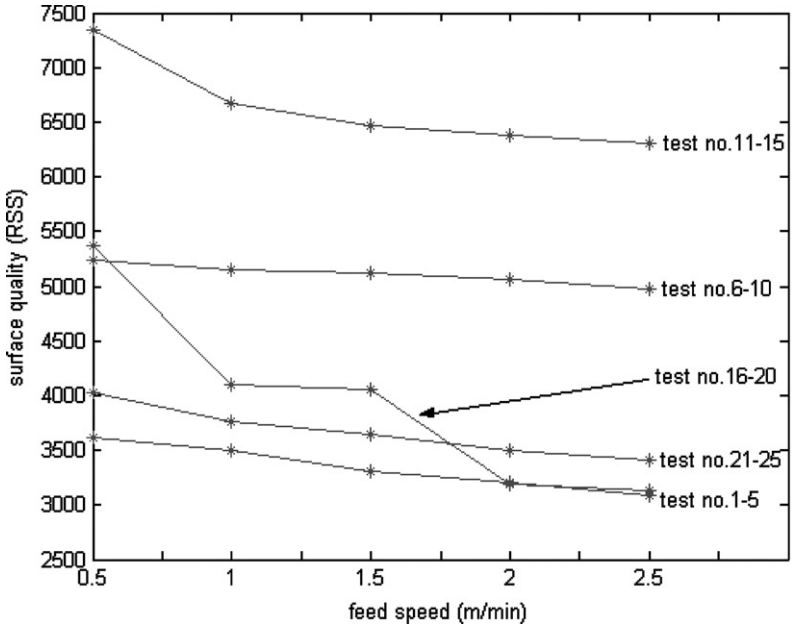

Fig. 14. Results of test nos. 1–25.

5.2. Discussion

The adaptive spline wavelet algorithm is performed for general and detailed vibration analysis. For general analysis, the frequency band of interest can be chosen. Although theoretical calculation of rotating and fundamental frequencies can provide their rough ranges in the frequency domain, the accurate identification is still needed with wavelet analysis, which is important to the feature extraction. However, although DWT is very efficient from a computational point of view, the dyadic disposition in scale is usually too coarse to correctly

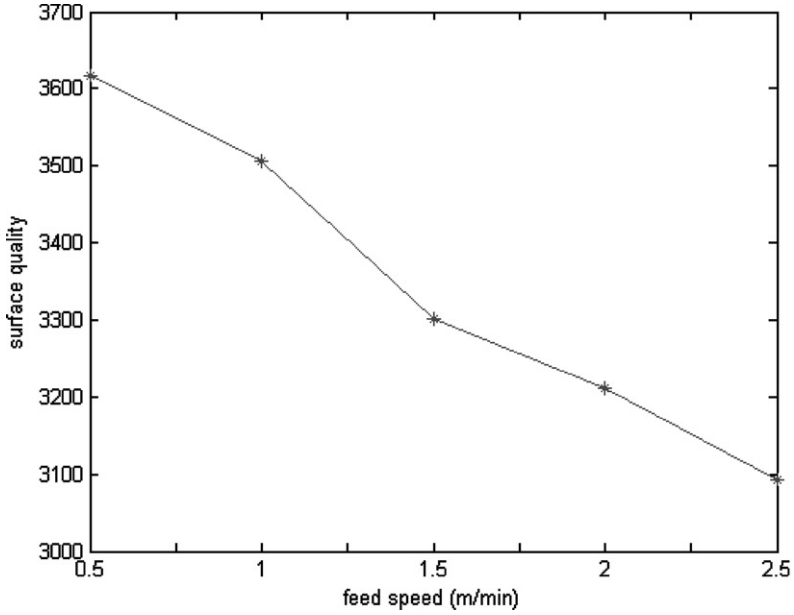

Fig. 15. Results of test nos. 1–5.

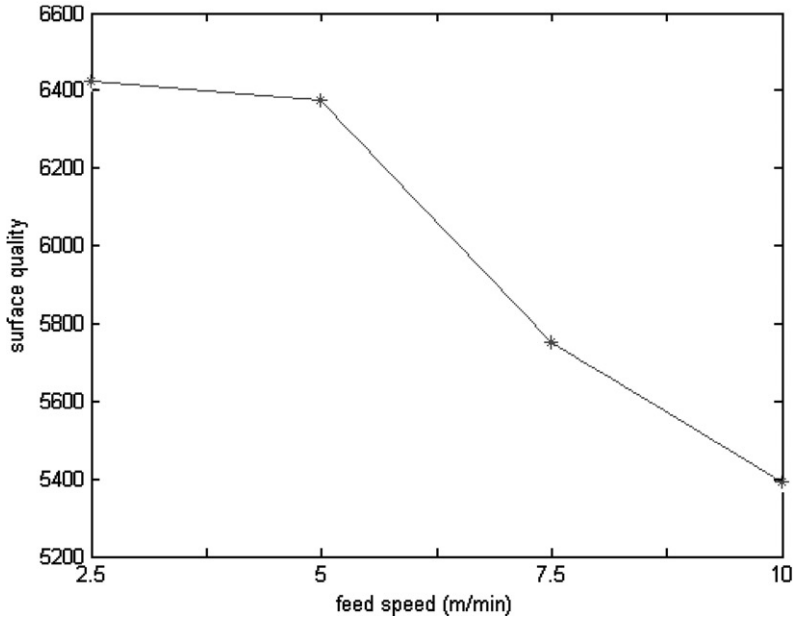

Fig. 16. Results of test nos. 26–29.

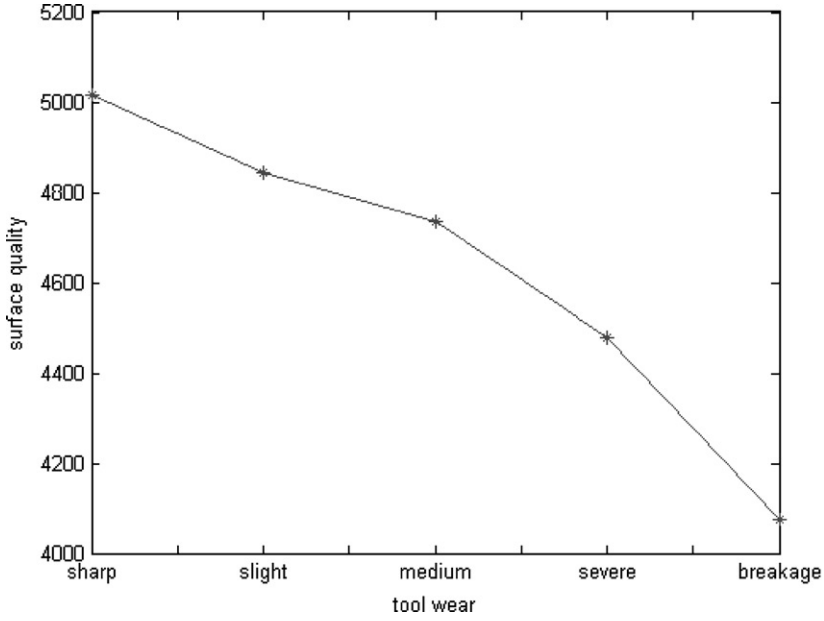

Fig. 17. Results of test nos. 30–34.

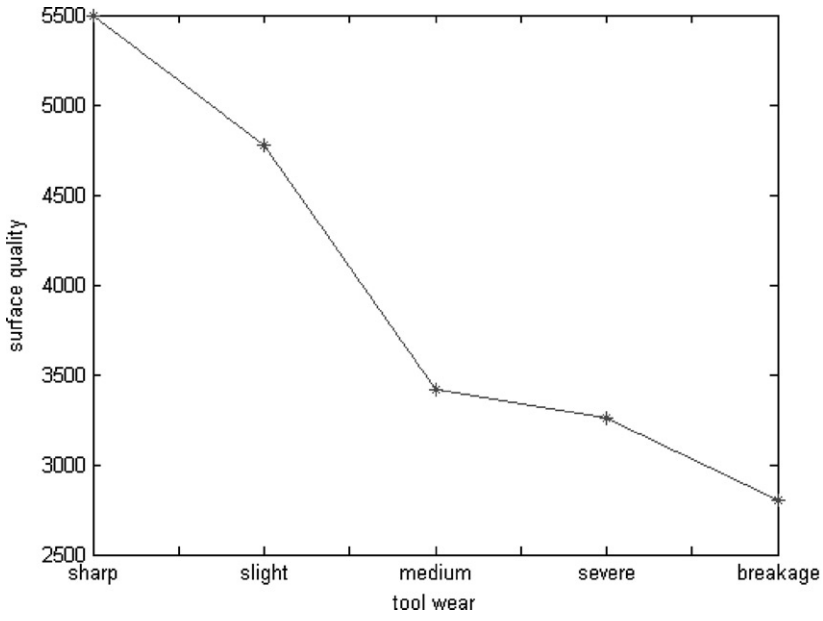

Fig. 18. Results of test nos. 35–39.

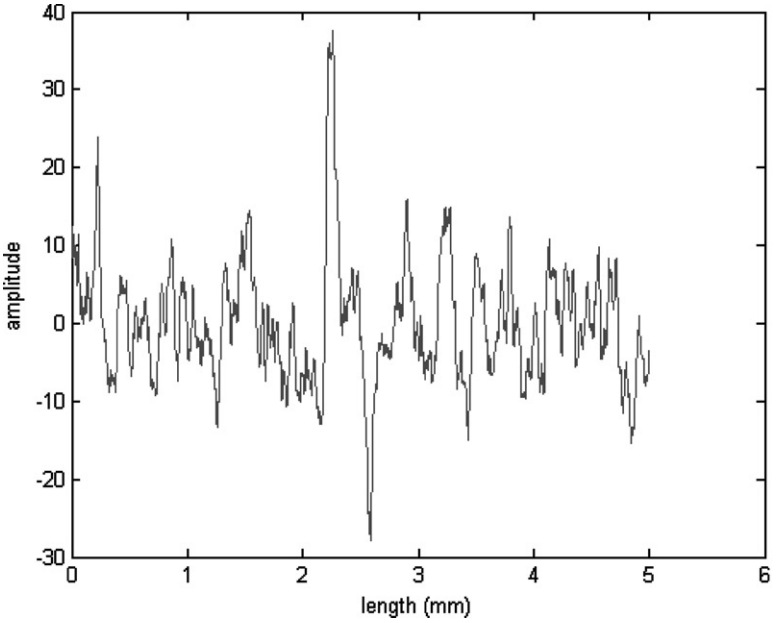

Fig. 19. An example of surface roughness profile corresponding to test no. 40.

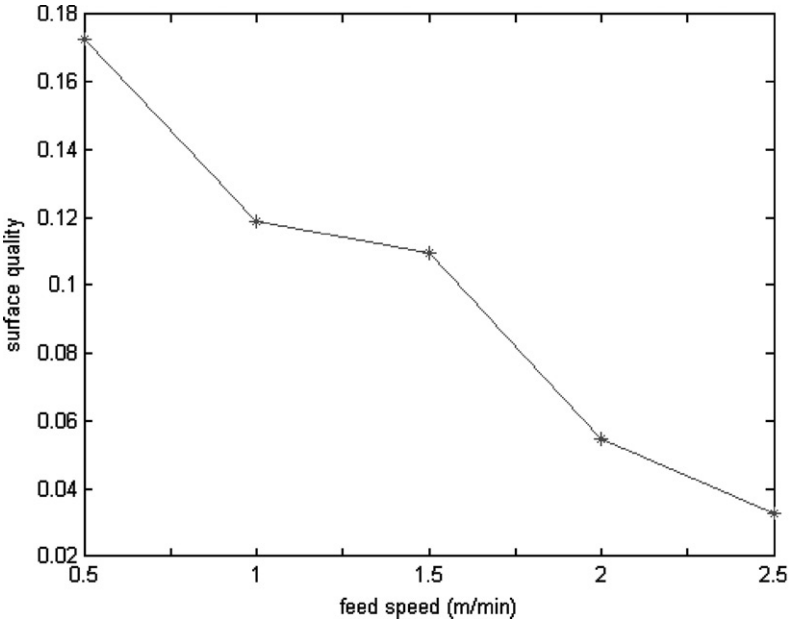

Fig. 20. Surface quality calculated from roughness measurement test nos. 40–44.

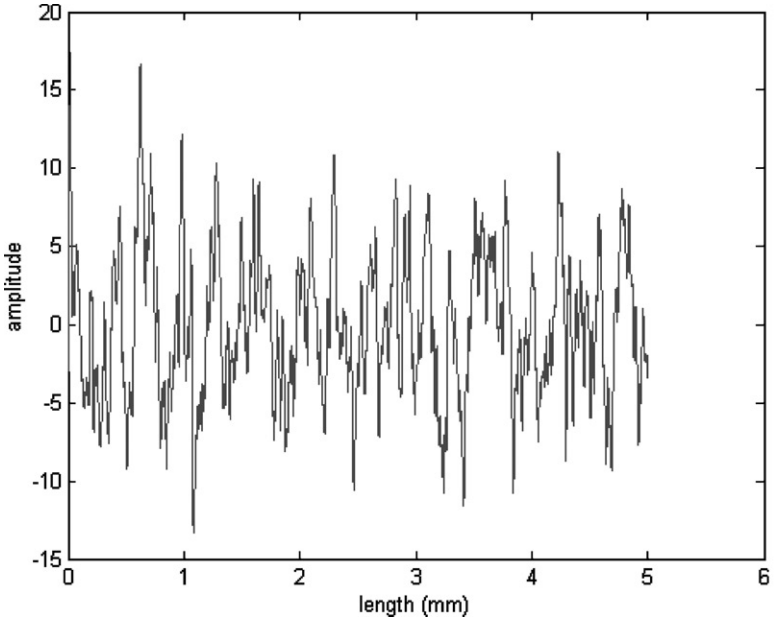

Fig. 21. An example of surface roughness profile corresponding to test no. 46.

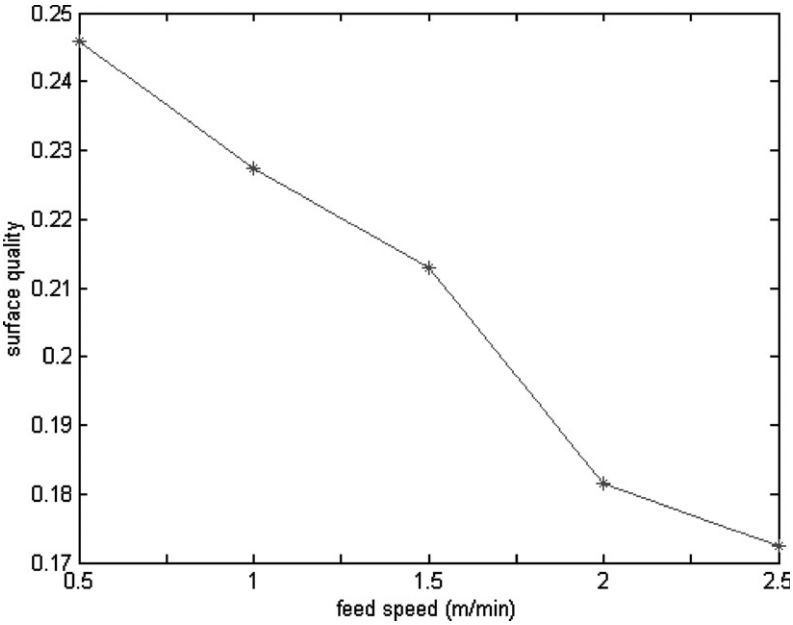

Fig. 22. Surface quality calculated from roughness measurement test nos. 45–49.

track the evolution of the WT coefficients through the scale levels, and only offers limited detailed information. This is shown in Fig. 5. For a further detailed analysis, an arbitrary fine scale analysis is used to decompose the signal into more detail as shown in Fig. 6. However, this is not adequate due to the low resolution at high frequencies. The development of an adaptive algorithm with a variable resolution (linear and non-linear), makes it possible to flexibly test the contribution of all possible frequency bands with varying bandwidth to surface quality (The time–frequency analysis with variable bandwidths distinguishes it from the STFT). This is based on the accurate identification of fundamental and rotating frequencies with high-resolution analysis, making use of good time–frequency localization property of the spline wavelet. The results show that RSS of wavelet power spectrum has a close relation to surface quality although the linear relation is not found, possibly because of measurement error.

Machine cutting experiments were carried out mainly varying two parameters: feed speed and tool wear, which are the factors influencing the surface quality. The recorded vibrations were analyzed using the adaptive algorithms. In comparison with the test results, actual surface roughness measurement is calculated by the widely used method of average roughness, and results are shown in Figs. 20 and 22 using the inverse proportion of average roughness.

Graphs of the actual measured results are similar to that of vibration analysis as shown in Figs. 14 and 15 (corresponding to Fig. 20). Although neither have perfect linear relationships, the quantification of surface quality is achieved from both actual measurement and vibration analysis. The results also match the theoretical calculation, in which feed speed is a major factor in terms of surface quality, and can be used to adjust the surface quality in general. This is the basis of this study, on which the on-line assessment of surface quality by vibration analysis can serve as a feedback signal to vary the process parameters, such as feed speed. The factor of tool wear to surface quality is also investigated (see Figs. 17 and 18) using the same technique, similar results are obtained as that of varying feed speed. Thus changing the cutter tool before detrimental wear states to affect surface quality is possible. The adaptive spline wavelet algorithm as well as its fast performance, can provide a very flexible analysis of vibration signals, and a method for feature extraction of surface quality. Operational speed of the fast algorithm also makes the proposed methodology suitable for real-time implementation on manufacturing applications with surface quality estimation of workpiece being used for process control.

6. Conclusions

The results show that a correlation exists between vibration and surface quality. Vibration signal representation with an adaptive spline wavelet algorithm for general and detailed analysis, provides a useful tool for the detection of vibration transients through time–frequency decomposition. Feature extraction with accurate identification of rotating and fundamental frequencies is based on vibration wavelet analysis, and the root sum square of power wavelet spectrum has been found to be a good indication of surface quality. The experimental results demonstrate that the change of the amplitude in the selective frequency bands reflects the quality of surface finish, regardless of varying feed speed or tool wear state. Results are compared with actual surface roughness measurement. Thus, surface quality can be estimated and quantified at an average level. The fast wavelet algorithm with quantitative calculation of surface quality

provides on-line assessment capability. These analysis techniques can be used to regulate and optimize the machine's feed speed, maintaining the appropriate spindle motor speed during cutting, or to change the cutter when wear states become detrimental. This will lead to a higher level of control and better machining rates while keeping dimensional integrity and surface finish within specification.

References

[1] H.W. Pollack, Tool Design, Prentice-Hall, Englewood Cliffs, NJ, 1988.
[2] H.Y. Feng, R.B. Mrad, Scanning-based intelligent routing strategies for solid wood, Proceedings of the 13th International Wood Machining Seminar, Vancouver, Canada, June 17–20, 1997, pp. 299–309.
[3] W.R.D. Wilson, W. Lee, Mechanics of surface roughening in metal forming processes, Transactions of the American Society of Mechanical Engineers, Journal of Manufacturing Science and Engineering 123 (2001) 279–283.
[4] T.I. Ei-Wardany, H.A. Kishawy, M.A. Eibestawi, Surface integrity of die material in high speed hard machining, Part 1: micrographical analysis, Transactions of the American Society of Mechanical Engineers, Journal of Manufacturing Science and Engineering 122 (2000) 620–631.
[5] T.I. Ei-Wardany, H.A. Kishawy, M.A. Eibestawi, Surface integrity of die material in high speed hard machining, Part 1: microhardness variations and residual stresses, Transactions of the American Society of Mechanical Engineers, Journal of Manufacturing Science and Engineering 122 (2000) 632–641.
[6] W.P. Fu, Y.M. Huang, X.L. Zhang, Q. Guo, Experimental investigation of dynamic normal characteristics of machined joint surfaces, Transactions of the American Society of Mechanical Engineers, Journal of Vibration and Acoustics 122 (2000) 393–398.
[7] P.R. Pagilla, B. Yu, Robotic surface finish processes: modeling control and experiments, Transactions of the American Society of Mechanical Engineers, Journal of Dynamic Systems Measurement and Control 123 (2001) 93–102.
[8] I.Y. Tumer, K.L. Wood, I.J. Busch-Vishniac, A mathematical transform to analyze part surface quality in manufacturing, Transactions of the American Society of Mechanical Engineers, Journal of Manufacturing Science and Engineering 122 (2000) 273–279.
[9] J. Orech, J. Zilinec, M. Kleskenova, I. Georgiev, R. Cisty, M. Babiak, Automatic measurement and control in woodworking Industry, in: B. Hruz, M. Cicel (Eds.), Possibility of Laser Exploitation in Measuring for Woodworking Industry, Pergamon Press, New York, 1988, pp. 75–77.
[10] R.L. Lemaster, J.B. Taylor, High speed surface assessment of wood and wood-based composites, Proceedings of the 14th International Wood Machining Seminar, Paris, France, September 12–19, 1999, pp. 479–488.
[11] R.L. Lemaster, F.C. Beall, The use of an optical profilometer to measure surface roughness in medium density fiberboard, Forest Products Journal 46 (11/12) (1996) 73–78.
[12] S. Fuchs, Opportunities of sensor techniques for inspection of wood materials and its impediments, Proceedings of the 13th International Wood Machining Seminar, Vancouver, Canada, June 17–20, 1997, pp. 289–298.
[13] T.D. Faust, Real time measurement of veneer roughness by image analysis, Forest Products Journal 37 (6) (1987) 34–40.
[14] F.E. Sherlock, Machine Woodworking Technology for Hand Woodworker, Stobart & Son, London, 1988.
[15] P. Koch, Wood Machining Processes, The Ronald Press Company, New York, 1964.
[16] U. Heisel, H. Krondorfer, Application of surface method for vibration analysis to CNC-routers, Proceedings of the 13th International Wood Machining Seminar, Vancouver, Canada, June 17–20, 1997, pp. 253–264.
[17] U. Heisel, H. Krondorfer, Surface method for vibration analysis in peripheral milling of solid wood, Proceedings of the 12th International Wood Machining Seminar, Kyoto, Japan, October 2–4, 1995, pp. 115–125.
[18] A.D. Dimarogonas, S. Haddad, Vibration for Engineers, Prentice-Hall, Englewood Cliffs, NJ, 1992.
[19] S. Conforto, T. D'Alessio, Spectral analysis for non-stationary signals from mechanical measurements: a parametric approach, Mechanical Systems and Signal Processing 13 (3) (1999) 395–411.

[20] J.C. Goswami, A.K. Chan, Fundamentals of Wavelets: Theory, Algorithms, and Application, Wiley, New York, 1999.
[21] D.E. Newland, An Introduction to Random Vibration, Spectral and Wavelet Analysis, Longman Scientific and Technical, New York, 1993.
[22] G. Dalpiaz, A. Rivola, Condition monitoring and diagnostics in automatic machines: comparison of vibration analysis techniques, Mechanical Systems and Signal Processing 11 (1) (1997) 53–73.
[23] G.Y. Luo, D. Osypiw, M. Irle, Application of time–scale gaussian wavelet based fast algorithm for vibration transient detection, Proceedings of the IEE Electronics and Communications Seminar on Time–scale and Time–frequency Analysis and Applications, London, UK, 29 February, 2000, pp. 16/1–16/7.
[24] W. Sweldens, The lifting scheme: a construction of second generation wavelets, SIAM Journal of Mathematical Analysis 29 (2) (1997) 511–546.
[25] A. Aldroubi, M. Unser, Wavelets in Medicine and Biology, CRC Press, Boca Raton, FL, 1996.
[26] I. Daubechies, Ten Lectures on Wavelet, SIAM, Philadelphia, PA, 1992.
[27] G. Strang, T. Nguyen, Wavelet and Filter Banks, Wellesley-Cambridge Press, Cambridge, 1996.
[28] C.K. Chui, An Introduction to Wavelets, Academic Press, Boston, 1992.
[29] F. Müller, P. Brigger, K. Illgner, M. Unser, Multiresolution approximation using shifted splines, IEEE Transactions on Signal Processing 46 (9) (1998) 2555–2558.
[30] M. Unser, P. Thévenaz, A. Aldroubi, Shift-orthogonal wavelet bases, IEEE Transactions on Signal Processing 46 (7) (1998) 1827–1836.
[31] M. Unser, P. Thévenaz, A. Aldroubi, Shift-orthogonal wavelet bases using splines, IEEE Signal Processing Letters 3 (3) (1996) 85–88.
[32] M. Unser, A. Aldroubi, M. Eden, B-spline signal processing: Part I: theory, IEEE Transactions on Signal Processing 41 (2) (1993) 821–833.
[33] M. Unser, A. Aldroubi, M. Eden, B-spline signal processing: Part II: efficient design and applications, IEEE Transactions on Signal Processing 41 (2) (1993) 834–848.
[34] M. Unser, A. Aldroubi, M. Eden, A family of polynomial spline wavelet transforms, Signal Processing 30 (1993) 141–162.
[35] M. Unser, T. Blu, Fractional splines and wavelets, SIAM Review 42 (1) (2000) 43–67.
[36] M. Unser, Splines: a perfect fit for signal and image processing, IEEE Signal Processing Magazine 16 (6) (1999) 22–38.
[37] M. Unser, Splines and wavelets for medical imaging, Proceedings of the Fourth IEEE EMBS Berder International Summer School on Biomedical Imaging, Ile de Berder, France, 17–24 June, 2000.
[38] W. Sweldens, Construction and Applications of Wavelets in Numerical Analysis. Ph.D. Thesis, Department of Computer Science, Katholieke Universiteit Leuven, Belgium, 1994.
[39] G. Zhu, G. Lei, G. Pan, On application of fast and adaptive periodic Battle–Lemarié wavelets to modeling of multiple lossy transmission lines, Journal of Computational Physics 132 (1997) 299–311.
[40] C.K. Chui, Wavelets: A Tutorial in Theory and Applications, Academic Press, New York, 1992.
[41] G.Y. Luo, D. Osypiw, M. Irle, Real-time condition monitoring by significant and natural frequencies analysis of vibration signal with wavelet filter and autocorrelation enhancement, Journal of Sound and Vibration 236 (3) (2000) 413–430.
[42] S.K. Tang, On the time–frequency analysis of signals that decay exponentially with time, Journal of Sound and Vibration 234 (2) (2000) 241–258.
[43] S. Hiziroglu, I. Baba, Surface roughness evaluation of medium density fibreboard manufactured in Malaysia, Journal of Tropical Forest Products 5 (1) (1999) 93–97.
[44] T. Akbulut, S. Hiziroglu, N. Ayrilmis, Surface absorption, surface roughness, and formaldehyde emmision of Turkish medium density fiberboard, Forest Product Journal 50 (6) (2000) 45–48.
[45] S. Hiziroglu, M. Graham, Effect of press closing time and target thickness on surface roughness of particleboard, Forest Product Journal 48 (3) (1998) 50–54.
[46] S. Hiziroglu, Surface roughness analysis of wood composites: a stylus method, Forest Product Journal 46 (7/8) (1996) 67–72.

[47] S. Suzuki, J. Kobayashi, T. Tochigi, H. Fukui, Machinability of medium density fibreboard, I: the effects of clearance angle depth of cut on machinability in end surface cutting, Mokuzai Gakkaishi 43 (9) (1997) 731–737.
[48] S. LI, M.A. Elbestawi, Fuzzy clustering for automated tool condition monitoring in machining, Mechanical Systems and Signal Processing 10 (5) (1996) 533–550.
[49] G.Y. Luo, D. Osypiw, M. Irle, Multi-body dynamics: monitoring & simulation techniques—II, in: H. Rahnejat, M. Ebrahim, R. Whalley (Eds.), Vibration Modelling and Identification with Fourier Transform, Wavelet Analysis and Least-squares Algorithm, Professional Engineering Publishing Limited, 2000, pp. 313–326.